



Synergistic fusion of phase unwrapping and speckle tracking methods for deriving surface velocity from interferometric SAR data

Journal:	<i>Geoscience and Remote Sensing Letters</i>
Manuscript ID:	draft
Manuscript Type:	Letters
Date Submitted by the Author:	n/a
Complete List of Authors:	Liu, Hongxing; Texas A&M University, Department of Geography Zhao, Zhiyuan; Vexcel Canada Inc, Research Scientist Jezek, Kenneth; The Ohio State University, Byrd Polar Research Center
Key Words:	Synthetic aperture radar, Velocity measurement, Interferometry, Motion measurement, Remote sensing, Ice

Synergistic Fusion of Phase Unwrapping and Speckle Tracking Methods for Deriving Surface Velocity from Interferometric SAR Data

Hongxing Liu, *Member, IEEE*, Zhiyuan Zhao, and Kenneth Jezek, *Associate Member, IEEE*

Abstract— This paper presents a technique to calibrate and unify disconnected fringe regions in an interferogram for the derivation of accurate surface velocity measurements. The interferogram from repeat-pass interferometric SAR data is often partitioned by shear margins of ice streams and other low-coherence zones into many small, disconnected fringe regions. Although these isolated fringe regions can be unwrapped separately, the unwrapped phase for each region is referenced to a different seed point. Our technique exploits absolute range offset measurements from the speckle tracking method to bridge the isolated fringe regions in the interferogram. In this way, the unwrapped phases in these regions can be calibrated into consistent surface displacement measurements with a common reference point. Using Radarsat interferometric data in Antarctica, we demonstrated that the synergistic fusion of the measurements from the phase unwrapping and speckle tracking methods can produce a two-dimensional velocity field with the best possible accuracy.

Index Terms— phase unwrapping, speckle tracking, interferometric SAR, data fusion.

I. INTRODUCTION

ICE velocity measurements are fundamentally important in studying glacial flow dynamics and ice sheet mass balance [1]–[3]. The repeat-pass interferometric data acquired by Synthetic Aperture Radar (SAR) sensors onboard ERS-1, ERS-2 and Radarsat satellites have been widely applied to measure surface motion speeds and directions [4]–[6]. The phase unwrapping method, first demonstrated by [7], has become the standard approach to processing interferometric data. The conventional phase unwrapping method allows for a high measurement accuracy of surface displacements at a fraction of the radar signal wavelength. However, the interferogram from repeat-pass interferometric SAR data is often partitioned by shear margins of ice streams and other

low-coherence zones into disconnected fringe regions. Although various phase unwrapping algorithms have been developed, these algorithms can only unwrap the isolated fringe regions separately, with different reference (seed) points. To utilize the fragmented phase information, these fringe regions need to be linked and calibrated with a common reference point. Furthermore, the phase unwrapping method only provides the surface motion component in the range direction. To achieve a two dimensional velocity field, the motion measurements in the azimuthal direction are required.

In this paper, we present a technique to bridge the isolated fringe regions in an interferogram by exploiting absolute range offset measurements from the speckle tracking method. This technique calibrates and unifies the unwrapped phases in the disconnected fringe regions with a common reference point. Using Radarsat interferometric SAR data for Antarctica, we demonstrate that the range displacement measurements from phase unwrapping method and the azimuth displacement measurements from speckle tracking method can be fused to produce a precise two-dimensional velocity field.

II. PHASE UNWRAPPING AND SPECKLE TRACKING

A SAR sensor measures both radar backscattering (brightness) information and distance information for the ground surface. The distance information is encoded in phase. The repeat-pass interferometric data pair consists of two complex radar images for the same scene acquired by a SAR sensor from almost the same geometry, but slightly different viewing angles during repeat passes. The phase differences in the two complex SAR images can be calculated by subtracting the phase in one image from the phase in the other. The phase difference image is known as an interferogram, which is a fine scale measurement of surface displacements in the radar line-of-sight (LOS) direction during two separate SAR passes. The phase differences in the interferogram wrap around in cycles of 2π , and the ambiguity of the correct multiple of 2π needs to be resolved for the absolute surface displacement measurements. Various phase unwrapping algorithms have been developed in the past decades, for example, the branch-cut algorithm [7], the weighted least-squares algorithm [8], and the region growing algorithm [9]. The phase measurement in the interferogram includes contributions from baseline, topography, and surface motion effects. The baseline effect

Manuscript received September 15, 2005. This work was supported by the the National Science Foundation (NSF) grant No. 0126149.

H. Liu is with the Department of Geography, Texas A&M University, College Station, TX 77843 USA (phone: 979-845-7998; fax: 979-862-4487; e-mail: liu@geog.tamu.edu).

Z. Zhao is with Vexcel Canada Inc., 20 Colonnade Road, Suite 110, Nepean, Ontario, K2E 7M6, Canada (e-mail: zhiyuan.zhao@vexcel.com).

K. Jezek is with Byrd Polar Research Center, The Ohio State University, Columbus, OH 43210, USA (e-mail: jezek@frosty.mps.ohio-state.edu).

can be removed with knowledge of SAR imaging geometry, while the topography effect can be removed by using a digital elevation model or using a double difference technique when more than two passes of SAR data are available [5], [10]. After the removal of the baseline and topography effects, the phase values in the interferogram are proportional to surface displacements in the LOS direction. To obtain the absolute surface motion measurements, an unknown constant phase, associated with the arbitrary selection of initial seed point for phase unwrapping, needs to be determined [2]:

$$\Phi_m = \Phi - \Phi_0 \quad (1)$$

where Φ_m is the surface motion induced phase in the LOS direction, Φ is the unwrapped phase after the removal of baseline and topography effects, and Φ_0 is the unknown constant phase to be solved.

Under the assumption that the ice flow vector is parallel to the ice surface, the radial LOS velocity can be projected into horizontal surface velocities in the range direction [5]:

$$V_r = \frac{\lambda}{4\pi T \sin(\beta + \alpha_r)} \Phi_m \quad (2)$$

where V_r is the surface motion velocity in the range direction, λ is the wavelength of radar signal, T is the time interval between acquisitions, β is the incidence angle, and α_r is the surface slope angle in the range direction. The geometry parameters of interferometry are illustrated in Fig. 1.

The speckle tracking method has been developed as an

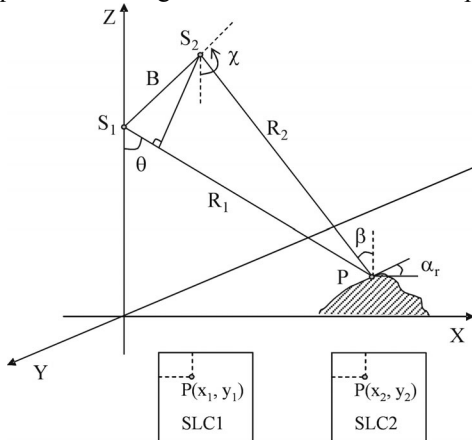


Fig. 1. Geometry of repeat-pass interferometry.

alternative approach to the processing of the repeat-pass interferometric SAR data for the surface velocity [1], [2], [6]. Speckle tracking method measures surface displacements by correlating and tracking image speckle pattern between two repeat-pass acquisitions. A correlation matching algorithm is commonly used to obtain both azimuth and range direction offsets based on the coherent speckle pattern of small chips of the SAR image pair [1], [2], [6]. Through oversampling of the correlation surface, the matching peak can be determined to a small fraction of a pixel spacing. The range offset δ_r and azimuth offset δ_a detected from cross-correlation matching include non-motion component contributed by the imaging geometry (parallel baseline and orbit squint angle) and

topography effect. The topography induced offsets only occur in the range direction and can be removed by using a digital elevation model. The geometry-induced terms in the range and azimuth offset can be modeled and removed using two linear equations [2], [6]:

$$d_r = \delta_r - (a_0 + a_1x + a_2y) \quad (3)$$

$$d_a = \delta_a - (b_0 + b_1x + b_2y) \quad (4)$$

where d_r and d_a are respectively the surface displacements in the range and azimuth directions measured in pixel, x and y are the range and azimuth coordinates of the slant range image, a_0 , a_1 , and a_2 are coefficients of the linear model for accounting for the geometry term in range direction, and, b_0 , b_1 , and b_2 are coefficients of the linear model for accounting for the geometry term in azimuth direction. The velocity components in range (V_r) and azimuth (V_a) directions can be calculated from the equations below:

$$V_r = \frac{d_r - B \cos(\chi - \theta)}{T \sin(\beta + \alpha_r)} \cdot S_r \quad (5)$$

$$V_a = \frac{d_a}{T \cos(\alpha_a)} \cdot S_a \quad (6)$$

where B is the length of the base line, χ is baseline angle, β is local incidence angle, θ is the radar look angle, α_r and α_a are terrain slopes respectively in the range and azimuth directions, S_r and S_a are pixel sizes respectively in range and azimuth directions, and T is the time interval between two acquisitions.

Two dimensional surface motion speed (s) and direction (ψ) can be calculated by the following equations:

$$s = \sqrt{V_r^2 + V_a^2} \quad (7)$$

$$\psi = \arctan\left(\frac{V_a}{V_r}\right) \quad (8)$$

The phase unwrapping method and speckle tracking method have their advantages and limitations [1], [2], [6]. The major advantage of the phase unwrapping method is that surface displacement measurements in the range direction have an intrinsically high resolution and accuracy. However, in fast-moving areas the high fringe rate of the interferogram may make the phase unwrapping impossible. The shear margins of the ice streams and outlet glaciers and other low-coherence zones induced by radar shadows, layover, and temporal decorrelation often fragment the interferogram into many small, disconnected fringe regions. Since the speckle tracking method is less sensitive to decorrelation and does not require phase unwrapping, it is able to provide displacement measurements farther into the shear margins and across areas of higher strain rate, where no phase measurements can be made. Furthermore, with a single interferometric SAR image pair, speckle tracking method can derive surface displacements in both range and azimuth directions, in contrast to the range-only displacement measurements of the phase unwrapping method. To make full use of the comparative advantages of both methods, the range motion component derived from the phase unwrapping method and the azimuth motion component derived from the speckle

matching method should be combined whenever possible [1], [2], [6].

III. LINKING DISCONNECTED FRINGE REGIONS

For an interferometric data pair, assume that the interferogram is partitioned into m fringe regions by highly decorrelated zones. Each fringe region can be individually unwrapped by selecting a seed point inside each region. As shown in (1), each fringe region has an unknown parameter Φ_0 , corresponding to its own reference seed point. There are m unknowns in total for the entire image. The mathematical formulation of our technique is based on the geometric relationship between the phase measurement and the range offset measurement for the same pixel.

The ranges R_1 and R_2 from the SAR sensor to the point P in the first and second passes (Fig. 1) can be expressed as linear functions of the range coordinates of the pixel in the slant range Single Look Complex (SLC) images:

$$R_1 = R_1^0 + x_1 S_r \quad (9)$$

$$R_2 = R_2^0 + x_2 S_r \quad (10)$$

where x_1 and x_2 are the range coordinates of the pixel in the first and the second images. R_1^0 and R_2^0 are ranges from the SAR sensor to the first pixel in the first and second images. S_r is the pixel size in the range direction. The range difference ΔR can be calculated by:

$$\Delta R = R_2 - R_1 = (R_2^0 - R_1^0) + S_r \delta_r \quad (11)$$

where $\delta_r = x_2 - x_1$ is the range offset of the pixel measured by the speckle tracking method.

For fringe region i , the range difference ΔR for a pixel can be correlated to its unwrapped phase Φ by the equation:

$$\Delta R = \frac{\lambda}{4\pi} (\Phi - \Phi_0^i) \quad (i = 1, \dots, m) \quad (12)$$

where Φ_0^i is a constant unknown value for fringe region i associated with the selected reference seed point in the phase unwrapping.

Combing (11) and (12), we obtain:

$$\Phi_0^i = \frac{4\pi}{\lambda} (R_2^0 - R_1^0) + (\Phi - \frac{4\pi}{\lambda} S_r \delta_r) \quad (i = 1, \dots, m) \quad (13)$$

In (13), R_1^0 , R_2^0 and S_r are constant values for SAR images, the unwrapped phase Φ is a relative measurement in unit of radian with respect to an arbitrary reference point, and the range offset δ_r is an absolute measurement in unit of pixel across the entire image frame. The phase measurement Φ is intrinsically more accurate than the range offset measurement δ_r derived from the speckle tracking method. Both the unwrapped phase Φ and the range offset δ_r contain the combined effects of the baseline, topography, and surface motion. Using the SAR imaging geometry and a digital elevation model, the baseline and topography effects can be removed from the phase and range offset measurements. After the removal, (13) is still valid since the baseline and topography effects in the phase and the range offset

measurements are canceled in the right side of the equation. Therefore, the unwrapped phase and the range offset terms in (13) can be treated as motion-only measurements. Since baseline and topography effects cause phase ramp and a high fringe rate in the interferogram, it is common practice to remove both baseline and topography effects in (13) to facilitate the phase unwrapping operation.

Assume that there are N pixels in fringe region i , the unknown parameter Φ_0^i for fringe region i can be estimated using the least-squares adjustment as:

$$\hat{\Phi}_0^i = \frac{4\pi}{\lambda} (R_2^0 - R_1^0) + \frac{1}{N} \sum_{j=1}^N (\Phi^j - \frac{4\pi}{\lambda} S_r \delta_r^j) \quad (i = 1, \dots, m) \quad (14)$$

where $\hat{\Phi}_0^i$ is the least-squares estimate for the unknown parameter, Φ^j and δ_r^j are respectively the unwrapped phase and range offset measurements for pixel j ($j=1, \dots, N$) in fringe region i . The estimate error in Φ_0^i can be quantified by the following formula:

$$\sigma_{\Phi_0^i}^2 = \frac{1}{N} \sigma_{\Phi}^2 + \frac{16\pi^2 S_r^2}{N\lambda^2} \sigma_{\delta_r}^2 \quad (15)$$

where σ_{δ_r} is the range offset measurement error from the speckle tracking method, and σ_{Φ} is the phase measurement error from the phase unwrapping method. The error in Φ_0^i is a systematic error for fringe region i introduced in the cross-region phase calibration. It is inversely proportional to the square root of N , the number of pixels in the fringe region.

As shown in (14), the isolated fringe regions can be unified by calibrating the unknown constant value Φ_0^i for each fringe region, based on the absolute range offset measurements from the speckle tracking method. After calibration, these fragmented fringe regions have accurate absolute phase measurements relative to a common reference, which can be readily utilized for the surface motion calculation.

IV. SYNERGISTIC FUSION

An interferometric SAR data pair over the Recovery Glacier, Antarctica is used to demonstrate our data fusion technique. The two SAR images in the interferometric pair were respectively acquired on September 21 and October 15, 1997 by the Radarsat-1 SAR sensor with the standard beam 7 (47° incidence angle). The parallel baseline is 206.3 m, and the perpendicular baseline is 215.8 m. A precision, phase preserving SAR processor was used to convert the raw radar signals into the single look complex (SLC) images. In the scene the tributary RAMP glacier flows from the top and merges into the Recovery Glacier, which moves from the left to the right (Fig. 2a). High backscatter returns are apparent in the shear margins of both the Recovery and the RAMP glaciers. The SLC images were co-registered at sub-pixel accuracy, and the level of coherence between the SLC image was calculated (Fig. 2b). Due to high deformations and ice crevasses, shear margins of the glaciers exhibit a very low coherence and appear in dark tone. With two co-registered

SLC images, the phase difference was determined on a pixel by pixel basis. With knowledge of the SAR imaging geometry and a digital elevation model [11], the effects of the baseline and topography were removed, resulting in a motion-only interferogram (Fig. 3). Clearly, the areas of slowly moving ice sheet denoted by *A* and *B* and the glacial floors (denoted by *C*, *D*, and *E*) between shear margins have quite sharp fringes. The five fringe regions *A*, *B*, *C*, *D*, and *E* are spatially separated by highly decorrelated shear margins, where the fringe pattern was completely destroyed and invisible.

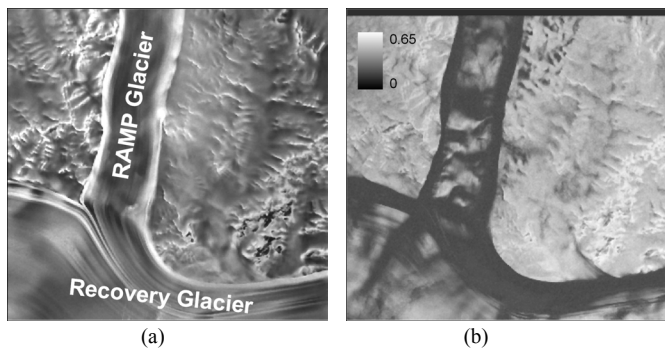


Fig. 2. Interferometric data over the Recovery Glacier, Antarctica. (a) SAR intensity image, and (b) Coherence image.

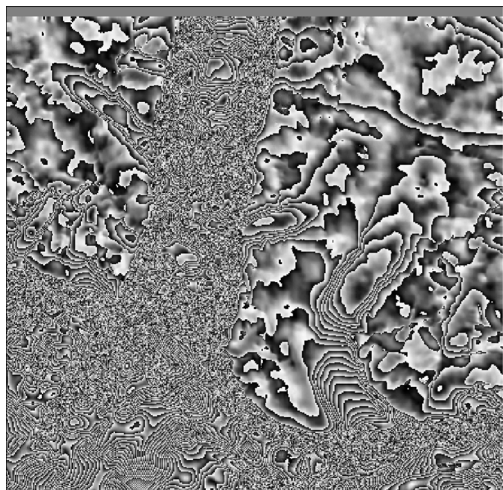


Fig. 3. Interferogram after removal of baseline and topography effects

By using the branch-cut algorithm [7] implemented in the Vexcel InSAR software package-Phase, the five fringe regions were separately unwrapped with five arbitrarily selected seed reference points (Fig. 4a). The location of the seed point for each fringe region is shown Fig. 4.

TABLE I

STATISTICS OF PHASE CALIBRATION CROSS FRINGE REGIONS				
Region	Seed Point	N	Φ_0^i (rad)	σ_{Φ_0} (rad)
<i>A</i>	200, 200	1994	17471	0.8
<i>B</i>	2500, 1000	5172 ²	17318	0.5
<i>C</i>	3363, 2545	287	20091	2.1
<i>D</i>	70, 2500	1607	19007	0.9
<i>E</i>	1420, 500	884	16559	1.2

Using the speckle tracking method, we computed range offsets. Then, the topography and geometry induced components in the range offsets are removed. With the

motion-only phase and motion-only range offset measurements, we calibrated the unknown parameter Φ_0^i ($i=1, \dots, 5$) for each fringe region using (14). The estimation error for the parameter (Table I) is also computed by using (15), in which $\sigma_s=0.02$ pixel, $\sigma_\phi=0.2$ rad, $S_r=8.1$ m. Overall, the estimation error is very small. For fringe region *C*, 2.1 radian error in Φ_0^i is equivalent to a velocity error of 0.14 m/year.

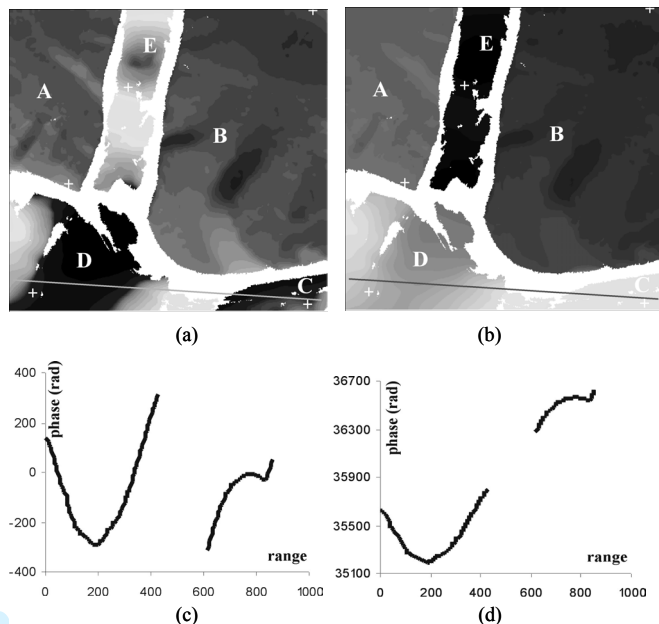


Fig. 4. Cross-region phase calibration for five isolated fringe regions. (a) Unwrapped phase before calibration, (b) unwrapped phase after calibration, (c) phase profile before calibration, and (d) phase profile after calibration. The plus signs in (a) and (b) indicate the locations of seed points, and lines indicate the position of profiles.

The unified absolute phase is shown in Fig. 4b. Now, the phase measurements of the spatially disconnected fringe regions are calibrated to a common reference point and hence consistent and comparable. Fig. 4c and 4d show the phase profiles before and after the phase calibration. The profile horizontally crosses through fringe regions *D* and *C*. Before the phase calibration, there is a steep discontinuity between two segments of unwrapped phase from regions *D* and *C*. After the phase calibration, the two segments of phase measurements are well aligned up.

The calibrated phase measurements are further converted into the range velocity by using (2). The range velocity gaps between the fringe regions are filled up by the less accurate range offset measurements from the speckle tracking method through (5). Speckle tracking method can provide displacement measurements farther into the shear margins and areas of high strain rate, because it is less sensitive to decorrelation than the phase unwrapping method.

We also computed the azimuth offsets by using the speckle tracking method. For the speckle tracking method, the accuracy of the azimuth offset measurements is significantly higher than that of range offset measurements. This is mainly because the azimuth resolution (about 5.4 m) is much better

the range resolution (about 8.1 m) in the SLC images. The azimuth offsets derived from the speckle tracking method contain the geometry and motion effects. The geometry effect is modeled and removed using (4). The motion-only azimuth offsets are further converted into azimuth velocity measurements using (6). By combining the range and azimuth velocity components through (7) and (8), we derive the ice flow speed and direction in two-dimensional space (Fig. 5).

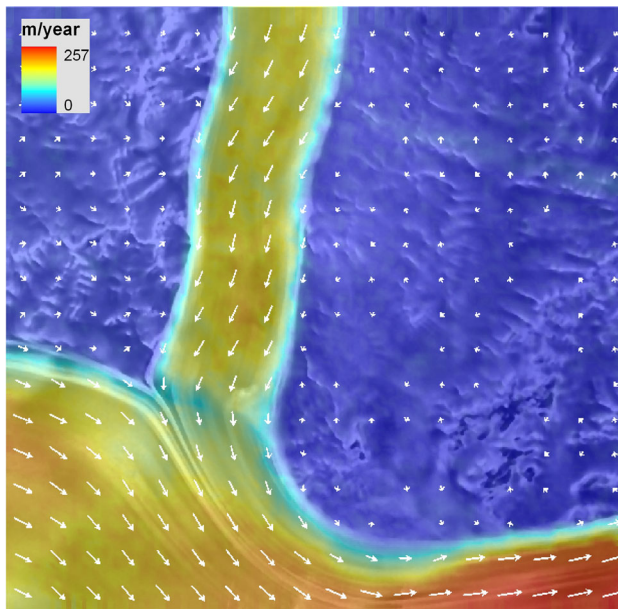


Fig. 5. A two dimensional velocity field produced by fusing phase unwrapping and speckle tracking measurements.

Clearly, the derived flow directions agree well with flow stripes observed from the SAR image. The spatial pattern of speed variation is consistent with the glacial features and the topography. The glacial channels have the fastest flow speed, up to 257 m/year. By comparing with ice flow stripes and independent velocity measurements, the derived flow directions are evaluated to be accurate within 5 degree, and the flow speeds are accurate to about 10-15 m/year [2].

V. CONCLUSION

We developed a technique to calibrate and correlate the disconnected fringe regions in an interferogram by utilizing the absolute range offset measurements from the speckle tracking method. Our technique is particularly useful for the areas with a high motion speed and for interferometric SAR data pairs with a long temporal baseline like Radarsat data, in which the shear margins of fast-moving glaciers and ice streams and other temporally decorrelated channels partition the interferogram into isolated fringe regions. An alternative method to calibrate disconnected fringe regions is to identify one or more velocity control points for each fringe region. However, velocity control points are frequently not available for all segmented regions. For our application example, we can use exposed rocks in fringe regions *A* and *B* as zero velocity control points, but no velocity control points can be identified for fringe regions *C*, *D*, and *E*. In this sense, our

technique greatly reduces the requirements for velocity control points. The surface displacement measurements derived from the phase unwrapping and speckle tracking are complementary. Our application example demonstrates that the synergistic fusion of the phase unwrapping and speckle tracking measurements spawns a two-dimensional velocity field with the best possible accuracy attainable with a single interferometric data pair.

REFERENCES

- [1] A.L. Gray, N. Short, K.E. Matter, and K.C. Jezek, 2001, "Velocities and Ice Flux of the Filchner Ice Shelf and its Tributaries determined from Speckle Tracking Interferometry," *Canadian Journal of Remote Sensing*, vol. 27, no. 3, pp. 193-206, 2001.
- [2] Z. ZHAO, Z., *Surface Velocities of the East Antarctic Ice Streams from Radarsat-1 Interferometric Synthetic Aperture Radar Data*. Ph.D. Dissertation, The Ohio State University, Columbus, Ohio, 2001
- [3] E. Rignot, "Mass balance of East Antarctic glaciers and ice shelves from satellite data," *Annals of Glaciology*, vol. 34, pp. 217-227, 2002.
- [4] R.M Goldstein, H. Engelhardt, B. Kamb, and R. Frolich, "Satellite radar interferometry for monitoring ice sheet motion: application to an Antarctic ice stream," *Science*, vol. 262, pp. 1525-1530, 1993.
- [5] R. Kwok and M. Fahnestock, "Ice sheet motion and topography from radar interferometry," *IEEE Transactions on Geoscience and Remote Sensing*, vol. 34, no. 1, pp. 189-199, 1996.
- [6] I. Joughin, "Ice-sheet velocity mapping: a combined interferometric and speckle-tracking approach," *Annals of Glaciology*, vol. 34, pp. 195-201, 2002.
- [7] R. M. Goldstein, H.A. Zebker, and C.L. Werner, "Satellite radar interferometry: two-dimensional phase unwrapping," *Radio Science*, vol. 23, no. 4, pp. 713-720, 1988.
- [8] D. Ghiglia, and L. Romero, "Robust two-dimensional weighted and unweighted phase unwrapping that uses fast transforms and iterative methods," *Journal of Optical Society of America*, vol. 11, no. 1, pp. 107-117, 1994.
- [9] W. Xu, and I. Cumming, "A region-growing algorithm for InSAR phase unwrapping," *IEEE Transactions on Geoscience and Remote Sensing*, vol. 37, no. 1, pp. 124-134, 1999.
- [10] I. Joughin, R. Kwok, and M. Fahnestock, "Estimation of ice-sheet motion using satellite radar interferometry: method and error analysis with application to Humboldt Glacier, Greenland," *Journal of Glaciology*, vol. 42, no. 142, pp. 564-575, 1996.
- [11] H. Liu, K.C. Jezek, and B. Li, "Development of Antarctic Digital Elevation Model by Integrating Cartographic and Remotely Sensed Data: A GIS-based Approach," *Journal of Geophysical Research*, vol. 104, no. B10, pp. 23,199-23,213, 1999.

Hongxing Liu (M'00) received his Ph.D. in geography in 1999 from the Ohio State University.

He is currently an assistant professor in the Department of Geography, Texas A&M University, College Station. His research interests include remote sensing, geographical information science, spatial data analysis, and environmental modeling. His recent research projects have been funded by NASA, NSF, and NOAA Sea Grant Program.

Zhiyuan Zhao received his Ph.D. in geodetic science in 2001 from the Ohio State University.

He is currently a research scientist in Vexcel Canada Inc. His research interests include remote sensing, SAR interferometry, and geo-spatial computation and algorithms.

Kenneth C. Jezek (A'92) received his Ph.D. in geophysics in 1980 from University of Wisconsin, Madison.

He is currently a professor at Byrd Polar Research Center and in the Department of Geology, the Ohio State University, Columbus. He was the director of the Byrd Polar Research Center, the Ohio State University during 1989-1999. Now, he leads a research team studying the earth's polar regions using satellite techniques.